

Novel Blue Phosphorescent Group 15 Compounds MR₃ (M = P, Sb, Bi; R = *p*-(N-7-Azaindoly)phenyl)

Youngjin Kang, Datong Song, Hartmut Schmider, and Suning Wang*

Department of Chemistry, Queen's University, Kingston, Ontario K7L 3N6, Canada

Received March 22, 2002

New blue phosphorescent organometallic compounds of group 15, M[*p*-C₆H₄(N-7-azain)]₃ with M = P (**1**), Sb (**2**), Bi (**3**) and 7-azain = 7-azaindoly, have been synthesized from the reaction of MCl₃ with Li[*p*-C₆H₄(N-7-azain)]. The crystal structures of these new compounds have been determined by single-crystal X-ray diffraction, which revealed that the group 15 elements in all three complexes are in a trigonal-pyramidal environment with the bond angles of C–M–C around the central atom decreasing from **1** to **3**, attributed to the diminution of s character of the M–C bond and the size increase of the central atom. All three compounds are blue luminescent. Both fluorescent and phosphorescent emissions ($\lambda_{\text{max}} = 371$ nm, $\lambda_{\text{max}} = 488$ nm) were observed for compound **1** at 77 K. In contrast, at 77 K, only phosphorescence was observed for compounds **2** and **3** ($\lambda_{\text{max}} = 483$ nm for **2**; $\lambda_{\text{max}} = 478$ nm for **3**), attributable to the increased heavy-atom effects. Experimental data and molecular orbital calculations (restricted Hartree–Fock methods) support the view that luminescences from all three compounds are ligand-based emissions with contributions from the lone-pair electrons of the central atom. The orange Bi(V) compound Bi[*p*-C₆H₄(N-7-azain)]₃Cl₂ (**4**) was obtained by the oxidation of **3** with PhI·Cl₂. Compound **4** displays a distorted-trigonal-bipyramidal structure and a weak phosphorescence at $\lambda_{\text{max}} = 510$ nm at 77 K, which is most likely caused by charge-transfer transitions from the chloride ligand to the Bi(V) center.

Introduction

Luminescent organic/organometallic complexes and the development of phosphors based on transition metals and main-group complexes have attracted much attention recently because of their potential applications in sensor technologies and photochemical and electroluminescent devices.^{1,2} In particular, a number of phosphorescent *d*-block heavy-metal inorganic and organometallic complexes, such as those of Pt(II) and Ir(III), have been demonstrated to be highly efficient emitters in OLEDs (organic light emitting devices).² The Pt(II) and Ir(III) metal centers in these compounds were demonstrated to play a key role in promoting singlet–triplet state mixing and, hence, phosphorescent emission. Although extensive research has been carried out on luminescent main-group compounds, most previous studies focused on the development of fluorescent chelated group 13 complexes based on 8-hydroxyquinoline,

7-azaindoly, and azomethine derivatives.³ Applications of phosphorescent main-group compounds in OLEDs have hardly been explored, due to the scarcity of suitable phosphorescent main-group compounds. Luminescence/phosphorescence has been reported previously⁴ in halides of main-group metals with an s² electronic configuration, such as Tl⁺, Pb²⁺, and Bi³⁺. These compounds are, however, not suitable for OLED ap-

(2) (a) Baldo, M. A.; O'Brien, D. F.; You, Y.; Shoustikov, A.; Sibley, S.; Thompson, M. E.; Forrest, S. R. *Nature* **1998**, *395*, 151. (b) Adachi, A.; Baldo, M. A.; Forrest, S. R.; Lamansky, S.; Thompson, M. E.; Kwong, R. C. *Appl. Phys. Lett.* **2001**, *78*, 1622. (c) Adachi, A.; Kwong, R. C.; Djurovich, P.; Adamovich, V.; Baldo, M. A.; Thompson, M. E.; Forrest, S. R. *Appl. Phys. Lett.* **2001**, *79*, 2082. (d) O'Brien, D. F.; Baldo, M. A.; Thompson, M. E.; Forrest, S. R. *Appl. Phys. Lett.* **1999**, *74*, 442. (e) Baldo, M. A.; Lamansky, S.; Burrow, P. E.; Thompson, M. E.; Forrest, S. R. *Appl. Phys. Lett.* **1999**, *75*, 4. (f) Kwong, R. C.; Sibley, S.; Dubovoy, T.; Baldo, M.; Forrest, S. R.; Thompson, M. E. *Chem. Mater.* **1999**, *11*, 3709. (g) Thompson, M. E.; Burrow, P. E.; Forrest, S. R. *Curr. Opin. Solid State Mater. Sci.* **1999**, *4*, 369. (h) Lamansky, S.; Djurovich, P.; Murphy, D.; Abdel-Razzag, F.; Lee, H.-E.; Adachi, C.; Burrows, P. E.; Forrest, S. R.; Thompson, M. E. *J. Am. Chem. Soc.* **2001**, *123*, 4304. (i) Lamansky, S.; Djurovich, P.; Murphy, D.; Abdel-Razzag, F.; Kwong, R.; Tsyba, I.; Bortz, M.; Mui, B.; Bau, R.; Thompson, M. E. *Inorg. Chem.* **2001**, *40*, 1704. (j) Sprouse, S.; King, K. A.; Spellane, P. J.; Watts, R. J. *J. Am. Chem. Soc.* **1984**, *106*, 6647. (k) Baldo, M. A.; Thompson, M. E.; Forrest, S. R. *Pure Appl. Chem.* **1999**, *71*, 2095.

(3) (a) Wang, S. *Coord. Chem. Rev.* **2001**, *215*, 79. (b) Schmidbauer, H.; Lettenbauer, J.; Wilkinson, D. L.; Müller, G.; Kumberger, O. *Z. Naturforsch.* **1991**, *46B*, 901. (c) Liu, S. F.; Seward, C.; Aziz, H.; Hu, N. X.; Popovic, Z.; Wang, S. *Organometallics* **2000**, *19*, 5709. (d) Chen, C. H.; Shi, J. *Coord. Chem. Rev.* **1998**, *171*, 161. (e) Hamada, Y.; Sano, T.; Fujita, M.; Fujii, T.; Nishio, Y.; Shibata, K. *Jpn. J. Appl. Phys.* **1993**, *32*, L511. (f) Hironaka, Y.; Nakamura, H.; Kusumoto, T. U.S. Patent 5,466,392, 1995. (g) Hamada, J.; Sano, K.; Fujita, M.; Fujii, T.; Nishio, Y.; Hamada, Y.; Shibata, K.; Kuroki, K. U.S. Patent 5,432,014, 1995. (h) Moore, C. P.; VanSlyke, S. A.; Gysling, H. J. U.S. Patent 5,484,922, 1996. (i) Burrow, P. E.; Sapochak, L. S.; McCarty, D. M.; Forrest, S. R.; Thompson, M. E. *Appl. Phys. Lett.* **1994**, *64*, 2718. (j) Matsumura, M.; Akai, T. *Jpn. J. Appl. Phys.* **1996**, *35*, 5357. (k) Kido, J.; Iizumi, Y. *Appl. Phys. Lett.* **1998**, *73*, 2721.

* To whom correspondence should be addressed. E-mail: wangs@chem.queensu.ca.

(1) (a) Tang, C. W.; VanSlyke, S. A. *Appl. Phys. Lett.* **1987**, *51*, 913. (b) Tang, C. W.; VanSlyke, S. A.; Chen, C. H. *J. Appl. Phys.* **1989**, *65*, 3610. (c) Hu, N.-X.; Esteghamatian, M.; Xie, S.; Popovic, Z.; Ong, B.; Hor, A. M.; Wang, S. *Adv. Mater.* **1999**, *11*, 1460. (d) Bulovic, V.; Gu, G.; Burrows, P. E.; Forrest, S. R.; Thompson, M. E. *Nature* **1996**, *380*, 29. (e) Balzani, V.; Juris, A.; Venturi, M.; Campagna, S.; Serroni, S. *Chem. Rev.* **1996**, *96*, 759. (f) Shen, Z.; Burrows, P. E.; Bulovic, V.; Forrest, S. R.; Thompson, M. E. *Science* **1997**, *276*, 2009. (g) Papkovski, D. B. *Sens. Actuators, B* **1995**, *29*, 213. (h) Ma, Y.; Che, C.-M.; Chao, H.-Y.; Zhou, X.; Chan, W.-H.; Shen, J. *Adv. Mater.* **1999**, *11*, 852. (i) Mills, A.; Lepre, A. *Anal. Chem.* **1997**, *69*, 4653. (j) Poterini, G.; Serpone, N.; Bergkamp, M. A.; Netzler, T. L. *J. Am. Chem. Soc.* **1983**, *105*, 4639. (k) Ma, Y.; Zhang, H.; Shen, J.; Che, C.-M. *Synth. Met.* **1998**, *94*, 245. (l) Baldo, M. A.; Thompson, M. E.; Forrest, S. R. *Nature* **2000**, *403*, 750. (m) Papkovski, D. B.; Ponomarev, G. V.; Kurochkin, I. N.; Korpela, T. *Anal. Lett.* **1995**, *28*, 2027.

plications because of their ionic character and low volatility. Phosphorescent organometallic compounds of main-group elements are most promising for OLED applications because, by tuning the ligand environment, the desired thermal stability and volatility could be achieved readily. Despite their potential, phosphorescent organometallic compounds of main-group metals remain scarce. Therefore, as the first step toward using phosphorescent main-group compounds as emitters in OLEDs, we carried out the investigation and the development of phosphorescent organometallic group 15 compounds.

Our investigation is based on the results of our recent study on group 13 complexes and organic molecules of 7-azaindole and its derivatives.^{5,6} We have observed that these molecules produce bright blue luminescence that is dominated by fluorescence.^{5,6} Phosphorescence from the previously reported group 13 compounds or organic compounds of 7-azaindole or its derivatives is extremely weak and negligible. We reasoned that, by binding heavy atoms such as Sb³⁺ and Bi³⁺ to 7-azaindole or its derivative ligands, it may be possible to promote phosphorescent emission from the ligands via heavy-atom effects. We have investigated several series of organometallic compounds of group 15 using a number of 7-azaindolylyl derivative ligands. Herein we report the results of our systematic investigation on three new group 15 compounds based on the new blue luminescent ligand *p*-(*N*-7-azaindolylyl)phenyl (*p*-C₆H₄(*N*-7-azain)).

Experimental Section

All experiments were carried out under a dry nitrogen atmosphere either in an inert-atmosphere drybox or using standard Schlenk techniques. Solvents were freshly distilled over appropriate drying reagents, and all Schlenk flasks were flame-dried under vacuum prior to use. All starting materials were purchased from Aldrich and used without further purification. ¹H, ¹³C, and ³¹P NMR spectra were recorded on a Bruker Avance 300 spectrometer operating at 300, 75.3, and 121.5 MHz, respectively. The ³¹P NMR spectrum was referenced relative to 85% phosphoric acid. Excitation and emission spectra were recorded on a Photon Technologies International QuantaMaster Model 2 spectrometer. Emission lifetime was measured on a Photon Technologies International Phosphorescent lifetime spectrometer, Timemaster C-631F, equipped with a xenon flash lamp and digital emission photon multiplier tube using a band path of 4 nm for excitation and 4 nm for

emission. Elemental analyses were performed by Canadian Microanalytical Service Ltd., Delta, British Columbia, Canada. Melting points were determined on a Fisher-Johns melting point apparatus.

Preparation of 1-Bromo-4-(*N*-7-azaindolylyl)benzene.

1,4-Dibromobenzene (3.99 g, 16.9 mmol), 7-azaindole (1 g, 8.46 mmol), potassium carbonate (1.17 g, 8.46 mmol), and cupric sulfate hydrate (0.1 g, 0.42 mmol) were mixed in a flask and heated at 210–220 °C for 6 h. After it was cooled to room temperature, the mixture was dissolved in CH₂Cl₂ (200 mL) and washed with H₂O. The organic layer was dried over MgSO₄, and all volatiles were removed under reduced pressure. The residue was purified by column chromatography using ethyl acetate/hexane (1:3) as eluent. The product was recrystallized from ethyl acetate/hexane in 43% yield. Mp: 86–87 °C. ¹H NMR in CDCl₃ (δ, ppm, 25 °C): 8.40 (dd, *J* = 4.8, 1.5 Hz, 1H, 7-azain), 8.01 (dd, *J* = 8.6, 1.5 Hz, 1H, 7-azain), 7.69, 7.68 (AA'BB'', *J*_{AB} = 5.4 Hz, 2H, 2H, phenyl), 7.05 (d, *J* = 3.9 Hz, 1H, 7-azain), 7.18 (dd, *J* = 8.7, 4.8 Hz, 1H, 7-azain), 6.67 (d, *J* = 3.9 Hz, 1H, 7-azain). ¹³C NMR in CDCl₃ (δ, ppm, 25 °C): 148.07, 144.38 (Ph), 138.02 (Ph), 133.09 (Ph), 129.91, 127.98, 125.95, 122.34, 120.21 (Ph), 117.63, 102.87. Anal. Calcd for C₁₃H₉N₂Br: C, 57.16; H, 3.30; N, 10.26. Found: C, 57.32; H, 3.35; N, 10.26.

Preparation of P[*p*-C₆H₄(*N*-7-azain)]₃ (1). 1-Bromo-4-(*N*-7-azaindolylyl)benzene (0.25 g, 0.91 mmol) was added to a 100 mL Schlenk flask containing 20 mL of THF, and the solution was cooled to –78 °C. A 0.68 mL portion of *n*-butyllithium (1.6 M, 1.09 mmol) in hexane was added slowly. After the solution was stirred for 1 h at –78 °C, 0.054 g (0.396 mmol) of PCl₃ dissolved in Et₂O (10 mL) was added via cannula. After the mixture was stirred for 1 h at –78 °C, it was warmed to ambient temperature and stirred for an additional 18 h. The solution was filtered over a medium-porosity glass frit packed with Celite to remove the LiCl. The solvent was removed *in vacuo*, and the residue was extracted with toluene. The toluene extract was concentrated to about 2 mL and was layered with hexane. Colorless crystals of **1** formed over a period of several days at –10 °C in 30% yield. Mp: 224–225 °C. ¹H NMR in CD₂Cl₂ (δ, ppm, 25 °C): 8.37 (dd, *J* = 4.8, 1.5 Hz, 1H, 7-azain), 8.03 (dd, *J* = 8.1, 1.8 Hz, 1H, 7-azain), 7.93, 7.64 (AA'BB'', *J*_{AB} = 7.8 Hz, 2H, 2H, phenyl), 7.61 (d, *J* = 3.9 Hz, 1H, 7-azain), 7.18 (dd, *J* = 7.8, 4.8 Hz, 1H, 7-azain), 6.71 (d, *J* = 3.6 Hz, 1H, 7-azain). ¹³C NMR in CDCl₃ (δ, ppm, 25 °C): 147.83, 144.07, 139.69 (ph), 135.67 (²*J*_{C–P} = 20.3 Hz, Ph), 135.23 (¹*J*_{C–P} = 11.14 Hz, Ph), 130.12, 128.36, 124.34 (³*J*_{C–P} = 7.3 Hz, Ph), 122.64, 117.55, 102.91. ³¹P NMR in CDCl₃ (δ, ppm, 25 °C): –6.490. Anal. Calcd for C₃₉H₂₇N₆P: C, 76.72; H, 4.42; N, 13.77. Found: C, 75.86; H, 4.45; N, 13.30.

Preparation of Sb[*p*-C₆H₄(*N*-7-azain)]₃ (2). SbCl₃ (0.2 g, 0.91 mmol) in THF (10 mL) was slowly added to the solution of Li[*p*-C₆H₄(*N*-7-azain)] (0.36 g, 1.83 mmol) in THF (20 mL) at –78 °C. This solution was allowed warmed to ambient temperature and stirred for 12 h. After the mixture was filtered through Celite, the solvent was removed *in vacuo* and the residue was extracted with toluene. The toluene extract was concentrated to about 5 mL and was layered with hexane (5 mL). Crystallization at –10 °C gave colorless crystals in 45% yield. Mp: 214–216 °C. ¹H NMR in CDCl₃ (δ, ppm, 25 °C): 8.40 (dd, *J* = 4.8, 1.5 Hz, 1H, 7-azain), 7.99 (dd, *J* = 7.8, 1.8 Hz, 1H, 7-azain), 7.84, 7.72 (AA'BB'', *J*_{AB} = 8.4 Hz, 2H, 2H, phenyl), 7.56 (d, *J* = 3.6 Hz, 1H, 7-azain), 7.16 (dd, *J* = 7.8, 4.8 Hz, 1H, 7-azain), 6.66 (d, *J* = 3.6 Hz, 1H, 7-azain). ¹³C NMR in CDCl₃ (δ, ppm, 25 °C): 148.01, 144.29, 139.78 (Ph), 138.04 (Ph), 136.26 (Ph), 129.81, 128.29, 124.78 (Ph), 122.44, 117.49, 102.69. Anal. Calcd for C₃₉H₂₇N₆Sb: C, 67.08; H, 3.89; N, 11.65. Found: C, 66.78; H, 4.24; N, 11.97.

Preparation of Bi[*p*-C₆H₄(*N*-7-azain)]₃ (3). BiCl₃ (0.08 g, 0.25 mmol) dissolved in THF (10 mL) was slowly added to a solution of Li[*p*-C₆H₄(*N*-7-azain)] (0.11 g, 0.59 mmol) in THF (20 mL) at –78 °C. The mixture was stirred for 1 h at –78 °C

(4) (a) Vogler, A.; Kunkely, H. *Top. Curr. Chem.* **2001**, *213*, 143. (b) Nikol, H.; Vogler, A. *J. Am. Chem. Soc.* **1991**, *113*, 8988. (c) Vogler, A.; Nikol, H. *Pure Appl. Chem.* **1992**, *64*, 1311. (d) Vogler, A.; Nikol, H. *Comments Inorg. Chem.* **1993**, *14*, 245. (e) Narayanaswamy, R.; Mayne, P. J.; Kirkbright, G. F. *J. Inorg. Nucl. Chem.* **1978**, *40*, 129. (f) Ranfagni, A.; Mugnai, D.; Bacci, M.; Viliiani, G.; Fontana, M. P. *Adv. Phys.* **1983**, *32*, 823. (g) Blasse, G. *Prog. Solid State Chem.* **1988**, *18*, 79. (h) Vogler, A.; Paukner, A.; Kunkely, H. *Coord. Chem. Rev.* **1990**, *97*, 285.

(5) (a) Liu, S. F.; Wu, Q.; Schmider, H. L.; Aziz, H.; Hu, N.-X.; Popovic, Z.; Wang, S. *J. Am. Chem. Soc.* **2000**, *122*, 3671. (b) Ashenhurst, J.; Wu, G.; Wang, S. *J. Am. Chem. Soc.* **2000**, *122*, 2541. (c) Liu, W.; Hassan, A.; Wang, S. *Organometallics* **1997**, *16*, 4257. (d) Wu, Q.; Esteghamatian, M.; Hu, N. X.; Popovic, Z.; Enright, G.; Breeze, S. R.; Wang, S. *Angew. Chem., Int. Ed.* **1999**, *38*, 985. (e) Ashenhurst, J.; Brancaloni, L.; Hassan, A.; Liu, W.; Schmider, H.; Wang, S.; Wu, Q.; Wang, S. *Organometallics* **1998**, *17*, 3186. (f) Gao, S.; Wu, Q.; Wu, G.; Wang, S. *Organometallics* **1998**, *17*, 4666. (g) Wu, Q. G.; Wu, G.; Brancaloni, L.; Wang, S. *Organometallics* **1999**, *18*, 2553. (h) Hassan, A.; Wang, S. *Chem. Commun.* **1998**, 211.

(6) (a) Wu, Q.; Hook, A.; Wang, S. *Angew. Chem., Int. Ed.* **2000**, *39*, 3933. (b) Song, D.; Wu, Q.; Hook, A.; Kozin, I.; Wang, S. *Organometallics* **2001**, *20*, 4683. (c) Wu, Q.; Lavigne, J. A.; Tao, Y.; D'Iorio, M.; Wang, S. *Chem. Mater.* **2001**, *13*, 71.

Table 1. Crystallographic Data

	Br-C ₆ H ₄ -azain	1	2	3	4
formula	C ₁₃ H ₉ N ₂ Br	C ₃₉ H ₂₇ N ₆ P	C ₃₉ H ₂₇ N ₆ Sb	C ₃₉ H ₂₇ N ₆ Bi·0.5Et ₂ O·0.2C ₆ H ₁₄	C ₃₉ H ₂₇ BiCl ₂ N ₆ ·CH ₂ Cl ₂
fw	273.13	610.64	701.42	842.41	944.47
space group	<i>P</i> 2 ₁ / <i>c</i>	<i>P</i> 2 ₁ / <i>c</i>	<i>P</i> $\bar{1}$	<i>P</i> $\bar{1}$	<i>P</i> $\bar{1}$
<i>a</i> , Å	4.0269(12)	13.784(3)	9.958(9)	15.354(6)	11.8115(19)
<i>b</i> , Å	23.489(7)	24.096(5)	13.178(12)	16.010(6)	13.789(2)
<i>c</i> , Å	11.600(4)	9.2284(18)	13.772(12)	18.127(7)	13.898(2)
α , deg	90	90	113.802(12)	109.589(7)	117.420(2)
β , deg	91.527(5)	93.043(5)	93.512(15)	98.344(7)	100.217(3)
γ , deg	90	90	102.154(16)	114.720(7)	103.054(3)
<i>V</i> , Å ³	1096.9(6)	3060.7(10)	1595(2)	3595(3)	1850.8(5)
<i>Z</i>	4	4	2	4	2
<i>D</i> _{calcd} , g cm ⁻³	1.654	1.325	1.461	1.557	1.695
<i>T</i> , K	298	298	298	298	298
μ , cm ⁻¹	37.18	1.30	9.03	49.45	50.91
2 θ _{max} , deg	56.76	57.26	56.78	56.66	56.64
no. of rflns measd	7800	22 026	10 561	26 062	13 318
no. of rflns used	2635	7260	7093	16 615	8447
no. of params	181	416	415	869	453
<i>R</i> (<i>I</i> > 2 σ (<i>I</i>))	<i>R</i> 1 ^a = 0.0571 w <i>R</i> 2 ^b = 0.1236	<i>R</i> 1 = 0.0630 w <i>R</i> 2 = 0.0759	<i>R</i> 1 = 0.0817 w <i>R</i> 2 = 0.1762	<i>R</i> 1 = 0.0551 w <i>R</i> 2 = 0.0764	<i>R</i> 1 = 0.0285 w <i>R</i> 2 = 0.0687
<i>R</i> (all data)	<i>R</i> 1 = 0.1356 w <i>R</i> 2 = 0.1459	<i>R</i> 1 = 0.3247 w <i>R</i> 2 = 0.1104	<i>R</i> 1 = 0.2151 w <i>R</i> 2 = 0.2133	<i>R</i> 1 = 0.1863 w <i>R</i> 2 = 0.0943	<i>R</i> 1 = 0.0353 w <i>R</i> 2 = 0.0704
GOF on F ²	0.859	0.779	0.805	0.698	0.982

$$^a R1 = \sum |F_o|^2 - |F_c|^2 / \sum |F_o|^2. \quad ^b wR2 = [\sum w(F_o^2 - F_c^2)^2 / \sum w(F_o^2)^2]^{1/2}, \quad w = 1/[\sigma^2(F_o^2) + (0.075P)^2], \quad \text{where } P = [\text{Max}(F_o^2, 0) + 2F_c^2]/3.$$

and for an additional 12 h at ambient temperature. The solvent was removed *in vacuo*, and the residue was extracted with CH₂Cl₂. The CH₂Cl₂ extract was concentrated to about 2 mL. Hexane was added to precipitate the colorless product in 70% yield. Compound **3** was recrystallized from Et₂O/hexane at -10 °C. Mp: 225–227 °C. ¹H NMR in CDCl₃ (δ , ppm, 25 °C): 8.39 (dd, *J* = 3.2, 1.8 Hz, 1H, 7-azain), 7.98 (dd, *J* = 8.9, 1.5 Hz, 1H, 7-azain), 8.00, 7.85 (AA'BB'', *J*_{AB} = 8.4 Hz, 2H, 2H, phenyl), 7.55 (d, *J* = 3.6 Hz, 1H, 7-azain), 7.15 (dd, *J* = 7.8, 4.8 Hz, 1H, 7-azain), 6.65 (d, *J* = 3.6 Hz, 1H, 7-azain). ¹³C-¹H NMR in CDCl₃ (δ , ppm, 25 °C): 153.21 (Ph), 148.22, 144.26, 139.43 (Ph), 138.95 (Ph), 129.76, 128.40, 126.54 (Ph), 122.39, 117.41, 102.50. Anal. Calcd for C₃₉H₂₇N₆Bi: C, 59.39; H, 3.43; N, 10.66. Found: C, 59.41; H, 3.54; N, 10.61.

Preparation of Bi[*p*-C₆H₄(*N*-7-azain)]₃Cl₂ (4**).** Compound **3** (0.1 g, 0.126 mmol) was dissolved in 10 mL of CH₂Cl₂. This solution was cooled to -78 °C. PhI·Cl₂ (0.041 g, 0.15 mmol) was added. After the mixture was stirred for 3 h at -78 °C, the solvent was removed *in vacuo*. The residue was extracted with CH₂Cl₂. The extract was concentrated to ca. 2 mL and was layered with Et₂O. Yellow-orange crystals of compound **4** formed over a period of several days at -10 °C in 76% yield. Mp: 213–215 °C dec. ¹H NMR in CDCl₃ (δ , ppm, 25 °C): 8.76, 8.20 (AA'BB'', *J*_{AB} = 8.4 Hz, 2H, 2H, phenyl), 8.42 (dd, *J* = 4.8, 1.5 Hz, 1H, 7-azain), 8.01 (dd, *J* = 8.1, 1.8 Hz, 1H, 7-azain), 7.60 (d, *J* = 3.9 Hz, 1H, 7-azain), 7.20 (dd, *J* = 7.8, 4.8 Hz, 1H, 7-azain), 6.72 (d, *J* = 3.6 Hz, 1H, 7-azain). ¹³C NMR in CDCl₃ (δ , ppm, 25 °C): 157.79 (Ph), 148.76, 144.55, 141.92 (Ph), 136.93 (Ph), 130.05, 127.63, 126.51 (Ph), 122.65, 118.06, 103.85. Anal. Calcd for C₃₉H₂₇N₆Cl₂Bi: C, 54.58; H, 3.14; N, 9.78. Found: C, 53.88; H, 3.17; N, 9.38. The low carbon content is due to the presence of a small amount of CH₂Cl₂ present in the sample that could not be completely removed by vacuum.

X-ray Crystallography Analysis. Single crystals of *p*-bromo(*N*-7-azaindoly)benzene were obtained from ethyl acetate/hexanes. Suitable single crystals of compound **1** were obtained from CH₂Cl₂/hexanes, those for **2** were obtained from toluene/hexanes, those for **3** were obtained from Et₂O/hexanes, and those for **4** were obtained from CH₂Cl₂/diethyl ether. All the crystals were mounted on glass fibers and coated with epoxy glue. All data were collected on a Siemens P4 X-ray diffractometer with a Bruker SMART CCD 1000 detector, with monochromated Mo K α radiation, operating at 50 kV and 30 mA at 25 °C. No significant decay was observed during the data collection. Data were processed on a Pentium PC using

Bruker AXS Windows NT SHELXTL software package (version 5.10).⁷ Neutral atom scattering factors were taken from Cromer and Waber.⁸ Empirical absorption correction was applied to all crystals. All structures were solved by direct methods. There are two independent molecules in the asymmetric unit of **3**. Diethyl ether and hexane molecules cocrystallized with compound **3**; dichloromethane molecules cocrystallized with compound **4**. The disordering of diethyl ether and dichloromethane molecules was modeled successfully. All non-hydrogen atoms were refined anisotropically. The positions of hydrogen atoms were calculated, and their contributions in structural factor calculations were included. The crystal data are summarized in Table 1. Selected bond lengths and angles for **1–4** are given in Table 2.

Result and Discussion

Synthesis and Structure of *p*-Br-C₆H₄(*N*-7-azaindoly). We have demonstrated previously that deprotonated 7-azaindole ligands are efficient blue luminescent emitters when bound to Al(III) or B(III) centers.⁶ We have also shown that organic 7-azaindoly derivatives such as 1,3,5-tris(*N*-7-azaindoly)benzene and 4,4-bis(*N*-7-azaindoly)biphenyl are promising bright blue emitters for OLEDs.⁶ We therefore decided to attach the *p*-C₆H₄(*N*-7-azain) ligand to a group 15 metal center. The precursor molecule for this ligand is *p*-bromo(*N*-7-azaindoly)benzene, which was obtained by the Ullmann condensation⁹ reaction of 7-azaindole with excess 1,4-dibromobenzene at 210–220 °C, in the presence of CuSO₄ and K₂CO₃ (as a catalyst and a bromide scavenger, respectively) (Scheme 1). *p*-Bromo(*N*-7-azaindoly)benzene is soluble in most organic solvents, is stable in air in both the solid state and solution, and is easily sublimable. It was fully characterized by ¹H

(7) SHELXTL NT Crystal Structure Analysis Package, Version 5.10; Bruker AXS, Analytical X-ray System, Madison, WI, 1999.

(8) Cromer, D. T.; Waber, J. T. *International Tables for X-ray Crystallography*; Kynoch Press: Birmingham, AL, 1974; Vol. 4, Table 2.2A.

(9) (a) Goodbrand, H. B.; Hu, N. X. *J. Org. Chem.* **1999**, *64*, 670. (b) Lindley, J. *Tetrahedron* **1984**, *40*, 1433. (c) Fanta, P. E. *Synthesis* **1974**, 1.

Table 2. Selected Bond Lengths (Å) and Angles (deg) for 1–4

Compound 1			
P(1)–C(1)	1.824(5)	P(1)–C(14)	1.827(4)
P(1)–C(27)	1.826(4)		
C(1)–P(1)–C(27)	101.5(2)	C(27)–P(1)–C(14)	100.75(19)
C(1)–P(1)–C(14)	102.1(2)		
Compound 2			
Sb(1)–C(37)	2.107(11)	Sb(1)–C(31)	2.194(10)
Sb(1)–C(25)	2.163(10)		
C(37)–Sb(1)–C(25)	96.0(4)	C(25)–Sb(1)–C(31)	94.9(4)
C(37)–Sb(1)–C(31)	99.2(3)		
Compound 3			
Bi(1)–C(24)	2.220(12)	Bi(2)–C(63)	2.261(12)
Bi(1)–C(37)	2.242(11)	Bi(2)–C(76)	2.276(10)
Bi(1)–C(11)	2.256(11)	Bi(2)–C(50)	2.293(10)
C(24)–Bi(1)–C(37)	95.1(4)	C(63)–Bi(2)–C(76)	90.9(4)
C(24)–Bi(1)–C(11)	94.9(4)	C(63)–Bi(2)–C(50)	95.1(4)
C(37)–Bi(1)–C(11)	92.9(4)	C(76)–Bi(2)–C(50)	95.7(4)
Compound 4			
Bi(1)–C(1)	2.212(4)	Bi(1)–Cl(1)	2.5861(11)
Bi(1)–C(27)	2.217(3)	Bi(1)–Cl(2)	2.6147(10)
Bi(1)–C(14)	2.223(4)		
Cl(1)–Bi(1)–Cl(2)	172.64(3)	C(1)–Bi(1)–Cl(1)	89.56(10)
C(14)–Bi(1)–Cl(2)	92.01(10)	C(27)–Bi(1)–Cl(1)	87.22(10)
C(1)–Bi(1)–C(27)	142.64(13)	C(14)–Bi(1)–Cl(1)	95.21(10)
C(1)–Bi(1)–C(14)	106.82(13)	C(1)–Bi(1)–Cl(2)	89.71(10)
C(27)–Bi(1)–C(14)	110.54(13)	C(27)–Bi(1)–Cl(2)	88.92(10)

NMR, ^{13}C NMR, and elemental analysis. Interestingly, it has a significantly lower melting point (86–87 °C) than those of related derivatives: i.e., 1-bromo-3,5-bis-(*N*-7-azaindolyl)benzene (214 °C) and 7-*N*-azaindole (105 °C). This could be rationalized by the lack of intermolecular interactions in the solid state. Accordingly, a single-crystal X-ray diffraction analysis was carried out to understand the solid-state nature of this molecule. The structure of *p*-bromo-(*N*-7-azaindolyl)benzene is shown in Figure 1. The bond lengths C(8)–N(2) and C(11)–Br (1) are 1.421(7) and 1.899(6) Å, respectively, which are similar to those of previously reported 7-azaindolyl compounds.⁶ The unit cell packing diagram given in Figure 1 shows that the molecules of *p*-bromo-(*N*-7-azaindolyl)benzene stack along the *a* axis but the distance between two adjacent molecules is more than 4.0 Å, which is too far to have an effective π – π stacking interaction. Perhaps, as a result, this compound has a low melting point.

Syntheses and Structures of Compounds 1–3. Addition of MCl_3 ($\text{M} = \text{P}, \text{Sb}, \text{Bi}$) to $\text{Li}[p\text{-C}_6\text{H}_4(\text{N-7-azaindolyl})]$, prepared from the reaction of *n*-BuLi and *p*-bromo-(*N*-7-azaindolyl)benzene at –78 °C, gives a white suspension. Standard workup and crystallization from toluene/hexane or diethyl ether/hexane gives $\text{M}[p\text{-C}_6\text{H}_4(\text{N-7-azain})]_3$ as a pure colorless crystalline solid in moderate yield (Scheme 1). Compounds **2** and **3** are air stable, but compound **1** slowly decomposes in both the solid state and solution in air over several weeks, changing color from colorless to yellow. All compounds are soluble in common organic solvents except pentane and hexane and have been fully characterized by ^1H NMR, ^{13}C NMR, elemental analyses, and X-ray diffraction analyses. The ^1H NMR spectra of all compounds show five characteristic chemical shifts due to the 7-azaindolyl group and a typical AA'BB'' spin coupling

pattern due to the phenyl rings. The ^{13}C NMR spectrum of compound **1** shows the expected coupling patterns of the phosphorus atom with the carbon atoms of the phenyl ring ($^2J_{\text{P-C}} = 20.3$ Hz, $^1J_{\text{P-C}} = 11.14$ Hz, $^3J_{\text{P-C}} = 7.3$ Hz), consistent with previously reported ^{13}C – ^{31}P coupling patterns in related compounds.¹⁰ Compound **1** displays a chemical shift at –5.96 ppm in the ^{31}P NMR spectrum, which is shifted upfield, compared to PPh_3 , perhaps due to the electron-donating properties of the 7-azaindolyl group. One significant change of physical properties from *p*-bromo-(*N*-7-azaindolyl)benzene to compounds **1–3** is melting points. The melting points of compounds **1–3** are in the range 214–225 °C, which are nearly 3 times that of *p*-bromo-(*N*-7-azaindolyl)benzene, attributable to the increased molecular weight of compounds **1–3**, relative to that of *p*-bromo-(*N*-7-azaindolyl)benzene.

The structures of **1–3** were unambiguously established by single-crystal X-ray diffraction analyses. Notably, there are two independent molecules in the asymmetric unit of **3**. As shown by Figure 2, these three compounds have a trigonal-pyramidal geometry, typical for organophosphorus(III) and organometallic compounds of Sb(III) and Bi(III). The average C–M–C ($\text{M} = \text{P}, \text{Sb}, \text{Bi}$) bond angles in these three compounds are 101.5(2), 96.7(4), and 94.1(4)°, respectively, which are similar to those of the corresponding MPh_3 ($\text{M} = \text{P}, \text{Sb}, \text{Bi}$) compounds.¹¹ The bond angles become smaller from the phosphorus compound to the bismuth compound, which can be attributed to the decreased *s* contribution to the hybrid valence orbitals of the central atom and the increased size of the central atom from P to Bi. The same trend was also observed previously in other MR_3 compounds. The C–M ($\text{M} = \text{P}, \text{Sb}, \text{Bi}$) bond lengths are 1.824(5)–1.827(4), 2.107(11)–2.194(10), and 2.220(12)–2.293(10) Å, respectively, for the three compounds, which are comparable to the bond lengths in similar known compounds.¹¹

The three 7-azaindolyl groups in compounds **1** and **3** are all oriented in the same direction in a propeller fashion, resulting in an approximate C_3 symmetry, while in compound **2**, one of the 7-azaindolyl groups points in the direction opposite to the other two. Compounds **2** and **3** have interesting spatial arrangements in the crystal lattice. As shown by Figure 3, in the crystal lattice molecules of **2** and **3** form an interlocked pair, resulting in a cage-like arrangement structure that has an approximate S_6 symmetry. The metal–metal separation distances between the two paired molecules are 7.684(9) Å (Sb) and 7.782(3) Å (Bi), respectively. The arrangement of the paired molecules of **3** in the crystal lattice is shown in Figure 4 (compound **2** shows a similar arrangement). Compound **1** does not have the same spatial arrangement. No cage-like pairs were found for compound **1**.

(10) (a) Mann, B. E. *J. Chem. Soc., Perkin Trans. 2* **1972**, 1, 30. (b) Wuyts, L. F.; Van De Vondel, D. F.; Van Der Kelen, G. P. *J. Organomet. Chem.* **1977**, 129, 163.

(11) (a) Daly, J. J. *J. Chem. Soc.* **1964**, 3799. (b) Bruckmann, J.; Krüger, C.; Lutz, F. *Z. Naturforsch.* **1995**, 50, 351. (c) Adams, E. A.; Kolis, J. W.; Pennington, W. T. *Acta Crystallogr., Sect. C* **1990**, 46, 917. (d) Hawley, D. M.; Ferguson, G. J. *J. Chem. Soc. A* **1968**, 2059. (e) Jones, P. G.; Blaschette, A.; Henschel, D.; Weitz, A. *Z. Kristallogr.* **1995**, 210, 377. (f) Silvestru, C.; Breunig, H. J.; Althaus, H. *Chem. Rev.* **1999**, 99, 3277. (g) Dunne, B. J.; Orpen, A. G. *Acta Crystallogr., Sect. C* **1991**, C47, 345.

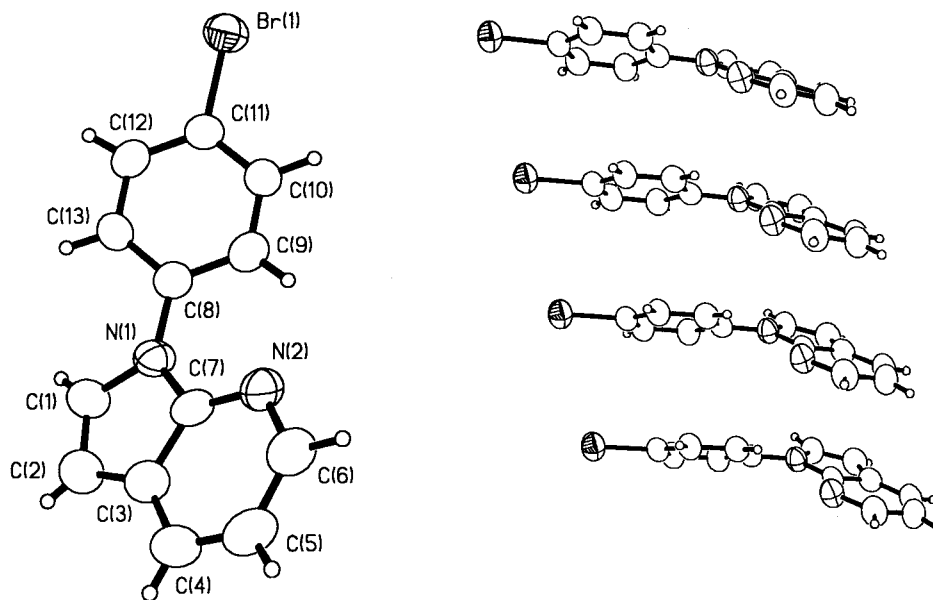
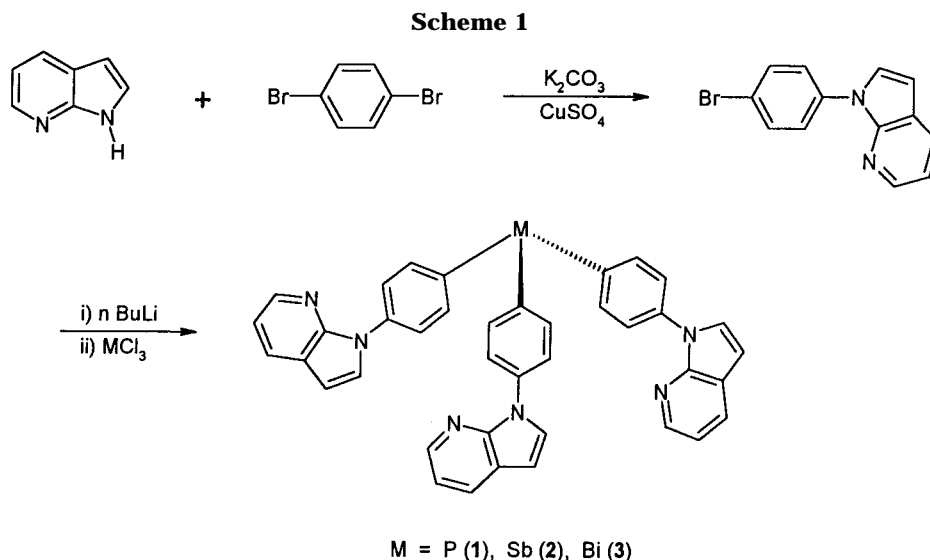


Figure 1. Diagrams showing (left) the molecular structure of *p*-bromo(*N*-7-azaindoly)benzene and (right) the stacking of *p*-bromo(*N*-7-azaindoly)benzene in the crystal lattice.



Synthesis and Structure of Compound 4, Bi[*p*-C₆H₄(*N*-7-azain)]₃Cl₂. To compare the luminescent properties of Bi(III) and Bi(V) compounds, we attempted the synthesis of Bi[*p*-C₆H₄(*N*-7-azain)]₅ by using Bi[*p*-C₆H₄(*N*-7-azain)]₃Cl₂ (**4**) as the precursor compound. The attempted synthesis and isolation of Bi[*p*-C₆H₄(*N*-7-azain)]₅ were unsuccessful due to its poor thermal stability (at ambient temperature, it reverts to compound **3**). The precursor compound **4** was obtained in good yield from the reaction of compound **3** with PhI·Cl₂. Compound **4** is yellow-orange and is stable in air in solution and the solid state. The structure of **4** was determined by X-ray diffraction analysis. As shown in Figure 5, the bismuth center has an approximate trigonal-bipyramidal coordination geometry with three organic ligands at equatorial positions and two chloride ligands at the axial positions. The Bi–Cl bond lengths are 2.5861(11) and 2.6147(10) Å, while C–Bi bond lengths are 2.212(4)–2.223(4) Å. Similar bond lengths were observed in¹² BiPh₃Cl₂ and Bi[*p*-C₆H₄(NMe₂)]₃Cl₂. The Cl(1)–Bi(1)–Cl(2) bond angle is 172.64(3)°, which

is about 7° off the ideal angle 180°, and the C–Bi–C bond angles are 142.64(13), 106.82(13), and 110.54(13)°, respectively. The distortion is due to the steric effect of the bulky organic ligands and the weak intermolecular interactions. As shown in Figure 5, each molecule of compound **4** interacts with an adjacent molecule through weak intermolecular Bi···Cl interactions to form a molecular pair with the intermolecular Bi···Cl separation distance being 3.614(1) Å. The Cl atom from the neighboring molecule approaches the equatorial plane of the Bi center, thus forcing the organic ligands away from an ideal trigonal-planar arrangement and resulting in a C–Bi–C angle that is much larger than the ideal angle 120°. Long Bi–Cl bonds are a common occurrence in bismuth compounds and have been well-documented previously.

(12) (a) Hawley, D. M.; Ferguson, G. *J. Chem. Soc. A* **1968**, 2539. (b) Hassan, A.; Breeze, S. R.; Courtenay, S.; Deslippe, C.; Wang, S. *Organometallics* **1996**, *15*, 5613. (c) Greenwood, N. N.; Earnshaw, A. *Chemistry of the Elements*; Pergamon Press: Oxford, U.K., 1984; Chapter 13, pp 659–665.

Table 3. Luminescence Data for the Ligand and Compounds 1–3

compd	UV-vis, nm ^a	excitation λ_{\max} , nm	emission λ_{\max} , nm	decay lifetime (τ , ms) ^b	conditions
<i>p</i> -Br-C ₆ H ₄ -(<i>N</i> -7-azain)	230, 264, 292	316 321	366 361 484	19(2)	CH ₂ Cl ₂ , 298 K CH ₂ Cl ₂ , 77 K
1	230, 276, 300	371 374 340 346	416 417 387 372 488	38(6) 0.69(6), 0.195(3)	solid, 298 K solid, 77 K CH ₂ Cl ₂ , 298 K CH ₂ Cl ₂ , 77 K
2	230, 274	414 344 329 327 421 461	465 474, 495 375 483 461 456, 491	78(10) 3.44(4) 0.597(8), 0.167(5) 0.45(1)	solid, 298 K solid, 77 K CH ₂ Cl ₂ , 298 K CH ₂ Cl ₂ , 77 K solid, 298 K solid, 77 K
3	230, 272	323 327 421 334	371 478 472 494	0.577(8), 0.093(8) 0.368(9), 0.098(5) 0.209(1)	CH ₂ Cl ₂ , 298 K CH ₂ Cl ₂ , 77 K solid, 298 K solid, 77 K
4	230, 278, 350–470 (very broad)	420	510	12.7(5)	CH ₂ Cl ₂ , 77 K

^a All data were collected for CH₂Cl₂ solutions ($[M] = 4.5 \times 10^{-5}$) at ambient temperature. ^b A reliable lifetime could not be obtained for the fluorescent emission due to the limitation of the instrument, which cannot measure lifetimes in the nanosecond regime.

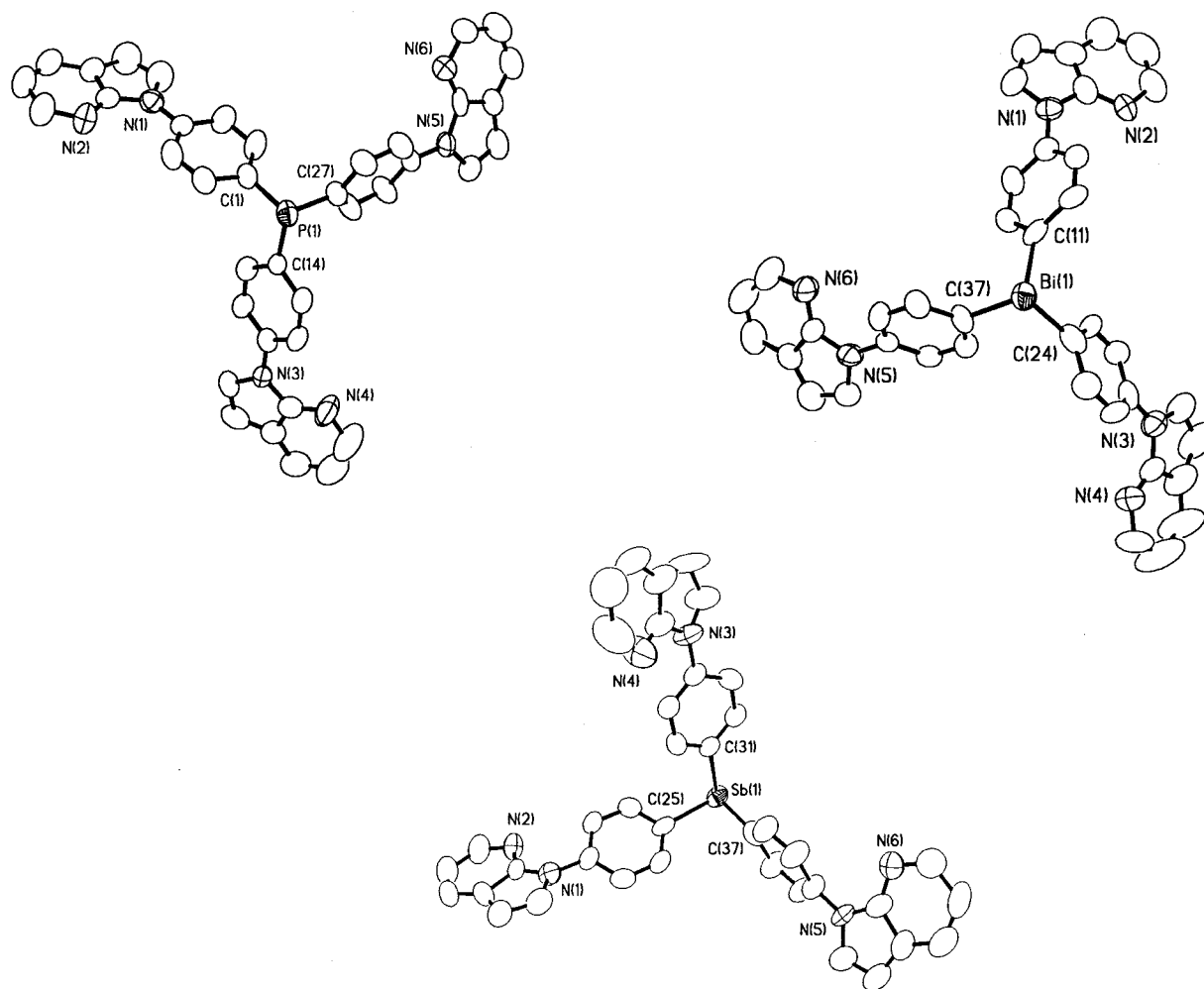


Figure 2. Molecular structures of **1** (top, left), **2** (bottom), and **3** (top, right) with 50% thermal ellipsoids and the labeling schemes for essential atoms.

Luminescent Properties. At 298 K the *p*-bromo-(*N*-7-azaindoly)benzene in CH₂Cl₂ solution has a broad fluorescent emission band with $\lambda_{\max} = 366$ nm. Similarly, compounds **1–3** display a broad fluorescent band ($\lambda_{\max} = 371–387$ nm) at 298 K. The emission lifetimes of fluorescence were not provided, because they could

not be measured accurately in our laboratory due to the limitation of the spectrometer. At 77 K, the frozen solution of *p*-bromo-(*N*-7-azaindoly)benzene displays two emission bands, an intense one at $\lambda_{\max} = 361$ nm and a weak one at $\lambda_{\max} = 484$ nm. The former is attributed to fluorescence, while the latter is attributed to phospho-

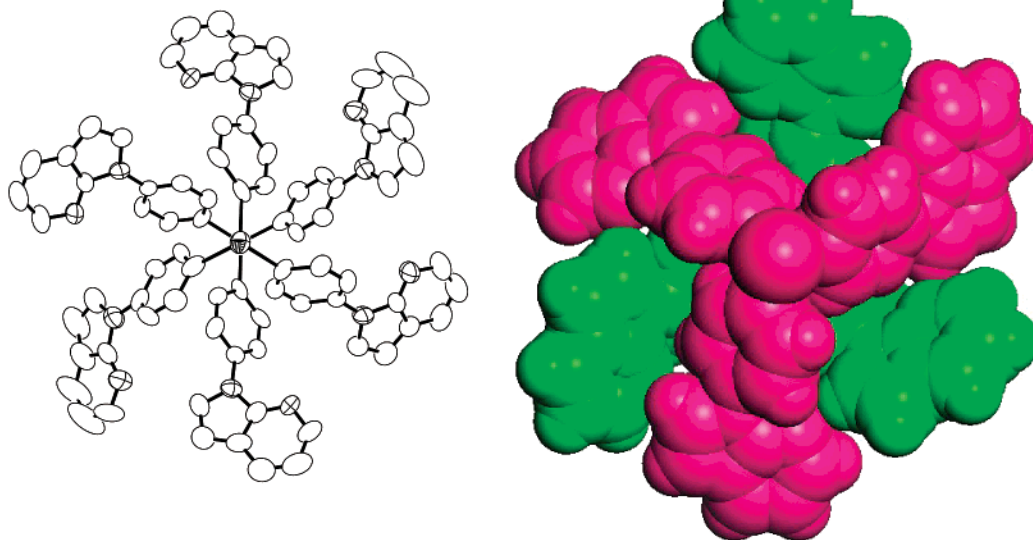


Figure 3. Diagrams showing (left) the interlocked pair of compound **3** in the crystal lattice, viewed down the Bi–Bi vector and (right) a space-filling model of the same view. The interlocked pair of **2** is similar.

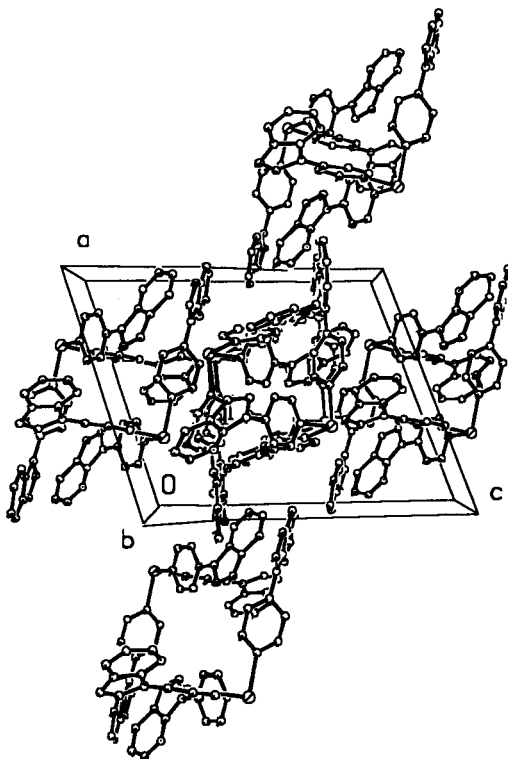


Figure 4. Unit cell packing diagram showing the arrangement of paired molecules of **3**. For clarity, solvent molecules and hydrogen atoms are omitted.

rescence, as supported by its long decay lifetime (19(2) ms). Heavy atoms have been known to promote the mixing of singlet and triplet states via spin–orbit coupling, hence promoting the emission from the triplet state (phosphorescence), the so-called *heavy-atom effect*.¹³ Since phosphorus is lighter than bromine, the attachment of *p*-(*N*-7-azaindoyl)phenyl to a phosphorus center is expected to disfavor the phosphorescent emis-

sion due to reduced heavy-atom effects, compared to that of *p*-bromo(*N*-7-azaindoyl)benzene. In fact, the emission spectrum of compound **1** in CH₂Cl₂ at 77 K has a fluorescent band ($\lambda_{\text{max}} = 372$ nm) and a phosphorescent band ($\lambda_{\text{max}} = 488$ nm) that are similar to those of *p*-bromo(*N*-7-azaindoyl)benzene. The decay lifetime (38(6) ms) of the phosphorescent band displayed by **1** is, however, twice that of *p*-bromo(*N*-7-azaindoyl)benzene, consistent with the reduced heavy-atom effect. Antimony and bismuth, in contrast, are much heavier than bromine and phosphorus. Therefore, for compounds **2** and **3**, the phosphorescent emission from the ligand is expected to be enhanced. Indeed, at 77 K in CH₂Cl₂ only the phosphorescent emission band (the fluorescent emission band is either not detectable or very weak and, thus, is negligible in comparison to the phosphorescent band) was observed for **2** ($\lambda_{\text{max}} = 483$ nm) and **3** ($\lambda_{\text{max}} = 478$ nm) (Figure 6), respectively, an indication that the intersystem crossing (or mixing) from the singlet state to the triplet state in both compounds is efficient. Further support for the enhanced phosphorescent emission in **2** and **3** is from the decay lifetime of the phosphorescent emission, which is 3.44(4) ms for **2** and 0.577(8) ms (the major component) for **3**, much shorter than those of *p*-bromo(*N*-7-azaindoyl)benzene and **1**. The trend of the phosphorescent decay lifetime decrease from **1** to **3** is consistent with the increased heavy-atom effect. The fact that the phosphorescent emission bands of *p*-bromo(*N*-7-azaindoyl)benzene and compounds **1–3** are in the same energy region made us believe they all originate from the same source: i.e., ligand-centered emission. In the solid state, *p*-bromo(*N*-7-azaindoyl)benzene has a bright fluorescent emission band with $\lambda_{\text{max}} = \sim 416$ nm at 298 and 77 K. In contrast, the solids of **1–3** at 298 and 77 K all display a weak blue phosphorescent emission band resembling those obtained in solution at 77 K. For compounds **1–3** a second decay component with a relatively short decay lifetime was detected at 77 K.

To understand the origin of luminescence displayed by compounds **1–3**, we performed *ab initio* calculations for all three compounds on the restricted Hartree–Fock

(13) (a) Drago, R. S. *Physical Methods in Chemistry*; W. B. Saunders: Philadelphia, PA, 1977; Chapter 5. (b) Masetti, F.; Mazzucato, U.; Galiazzi, G. *J. Lumin.* **1971**, *4*, 8. (c) Werner, T. C.; Hawkins, W.; Facci, J.; Torrisi, R.; Trembath, T. *J. Phys. Chem.* **1978**, *82*, 298.

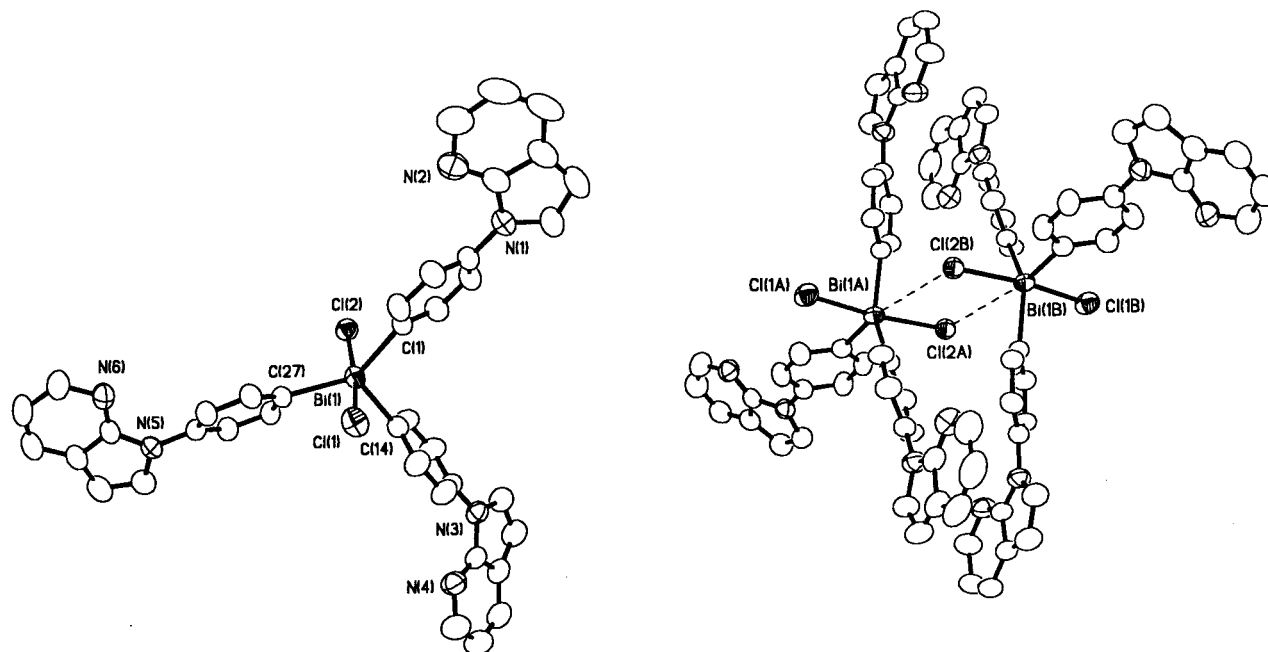


Figure 5. Diagrams showing (left) the molecular structure of **4** with 50% thermal ellipsoids and labels for important atoms and (right) intermolecular Bi...Cl interactions of **4**.

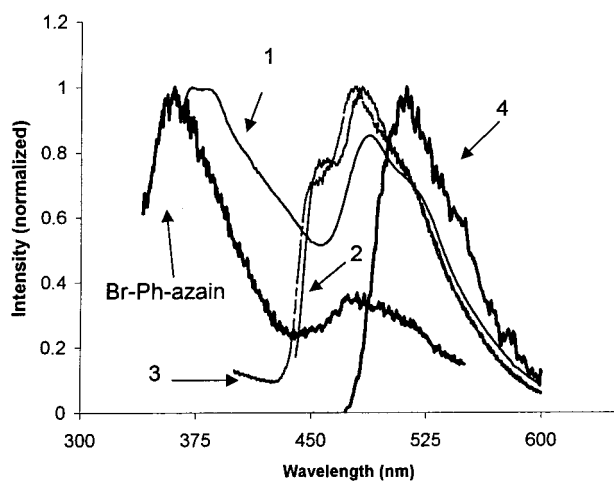


Figure 6. Emission spectra of *p*-bromo(*N*-7-azaindoly)benzene and compounds **1–4** at 77 K in CH_2Cl_2 .

(RHF) level using a standard split-valence polarized (6-31G*) basis set, employing the Gaussian 98 suite of programs.¹⁴ The geometric parameters employed in the calculations were from crystal structure data. MO calculations for **1** and **2** were carried out successfully, but no meaningful results could be obtained for compound **3**, mostly due to the large number of atomic orbitals involved. Figure 7 shows the surfaces (where the orbital attains values of ± 0.05 au) of highest

occupied molecular orbitals (HOMO's), second HOMO's, lowest unoccupied molecular orbitals (LUMO's) and second LUMO's for the compounds **1** and **2** along with the orbital energy for each level. As one may see, the HOMO's of both compounds involve π orbitals localized on the ligands. However, for the phosphorus compound **1**, the HOMO is dominated by the lone-pair orbital of the phosphorus atom. In contrast, the lone-pair orbital contribution to the HOMO level for the antimony compound **2** is much less, compared to the π orbital contributions from the ligands. The second HOMO of **1** consists of entirely ligand-based π orbitals. There is a considerable lone-pair contribution in the second HOMO of compound **2**. The LUMOs and second LUMOs for both compounds are π^* orbitals with contributions nearly entirely from the ligands. The HOMO–LUMO energy gaps for both compounds are nearly identical. The results of MO calculations provide further support to the conclusion that the luminescence observed in **1–3** is indeed due to $\pi \rightarrow \pi^*$ transitions with lone-pair contributions from the central atom. The precise origin of the two decay components has not been understood.

The Bi(V) center in compound **4**, $\text{Bi}(p\text{-C}_6\text{H}_4\text{-}N\text{-7-azaindoly})_3\text{Cl}_2$, does not have the lone-pair electrons. The removal of the lone-pair contribution to the HOMO level certainly should lead to the decrease of the HOMO energy level, hence widening the HOMO–LUMO gap, compared to compound **3**. The fact that compound **4** only displays a very weak emission band ($\lambda_{\text{max}} = 510$ nm) that is at much lower energy than that of **3**, with a decay lifetime (12.7(5) ms) that is much longer than that of **3** seems to indicate that the luminescence of **4** is not from $\pi \rightarrow \pi^*$ transitions centered on the ligands but is very likely from charge-transfer transitions from the chloride ligand to the Bi(V) center. The UV–vis spectrum of **4** in CH_2Cl_2 has a weak and broad absorption band (350–470 nm). Because the same absorption band is absent in compounds **1–3**, we believe that it is caused by a charge-transfer transition from chlorine to bismuth(V).

(14) Frisch, M. J.; Trucks, G. W.; Schlegel, H. B.; Scuseria, G. E.; Robb, M. A.; Cheeseman, J. R.; Zakrzewski, V. G.; Montgomery, J. A., Jr.; Stratmann, R. E.; Burant, J. C.; Dapprich, S.; Millam, J. M.; Daniels, A. D.; Kudin, K. N.; Strain, M. C.; Farkas, O.; Tomasi, J.; Barone, V.; Cossi, M.; Cammi, R.; Mennucci, B.; Pomelli, C.; Adamo, C.; Clifford, S.; Ochterski, J.; Petersson, G. A.; Ayala, P. Y.; Cui, Q.; Morokuma, K.; Malick, D. K.; Rabuck, A. D.; Raghavachari, K.; Foresman, J. B.; Cioslowski, J.; Ortiz, J. V.; Stefanov, B. B.; Liu, G.; Liashenko, A.; Piskorz, P.; Komaromi, I.; Gomperts, R.; Martin, R. L.; Fox, D. J.; Keith, T.; Al-Laham, M. A.; Peng, C. Y.; Nanayakkara, A.; Gonzalez, C.; Challacombe, M.; Gill, P. M. W.; Johnson, B. G.; Chen, W.; Wong, M. W.; Andres, J. L.; Head-Gordon, M.; Replogle, E. S.; Pople, J. A. *Gaussian 98*, revision A.6; Gaussian, Inc.: Pittsburgh, PA, 1998.

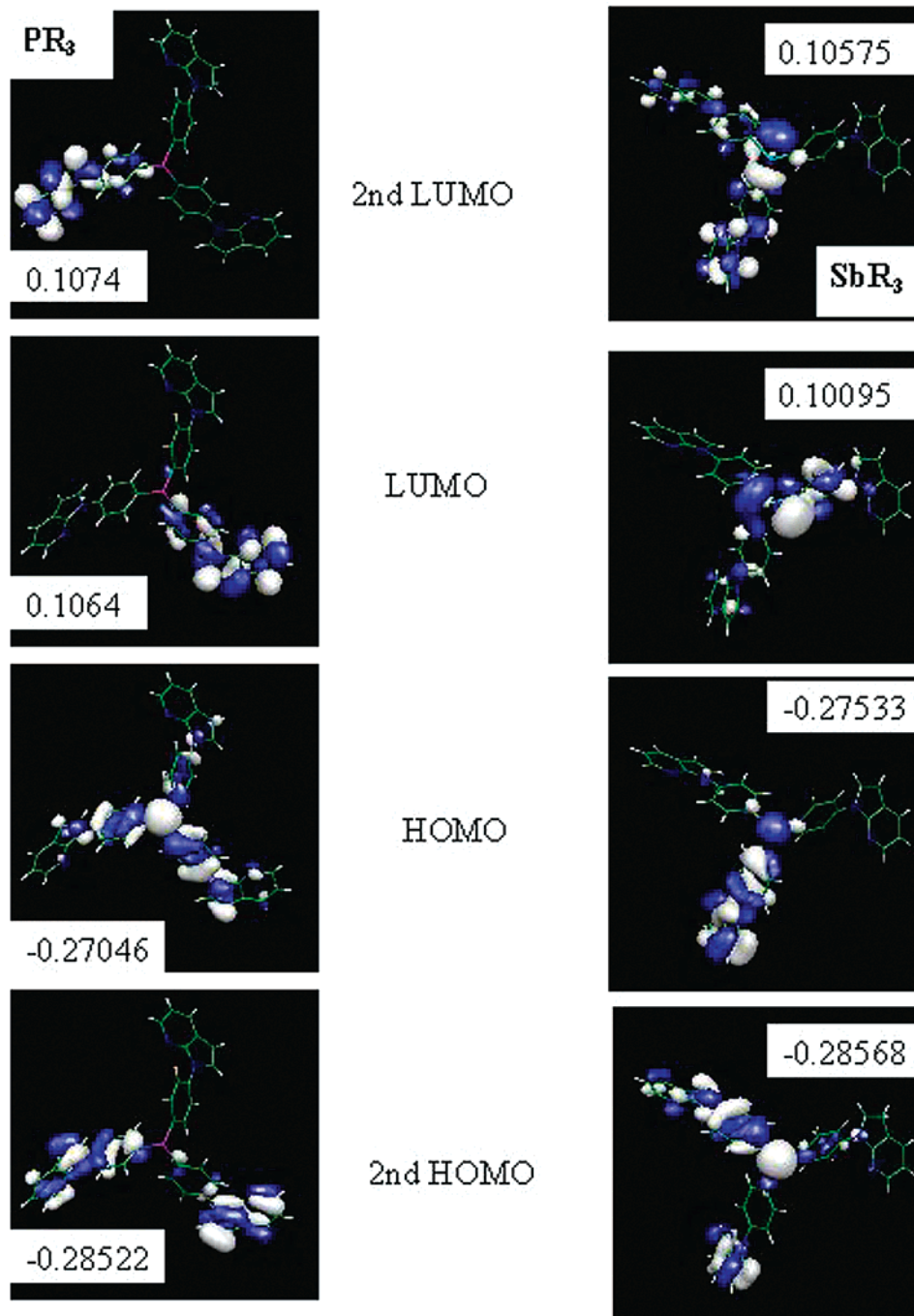


Figure 7. Diagram showing the surfaces and energies of HOMOs, 2nd HOMOs, LUMOs, and 2nd LUMOs for **1** and **2**.

The $\pi \rightarrow \pi^*$ transitions observed in **1–3** are likely quenched by this charge-transfer transition in **4**.

Due to the low phosphorescent emission intensity and long decay lifetimes of compounds **1–3** in the solid state at ambient temperature, we believe that these compounds are not suitable as emitters in OLEDs. Nonetheless, our investigation established that it is possible to enhance the phosphorescent emission centered on an organic ligand by incorporating appropriate main-group-metal centers. The incorporation of a main-group-metal center into the ligand also greatly increases the melting point of the compound. Modification of the luminescent ligand and the coordination environment around the central atom could lead to further improvement of the

phosphors and their ultimate use in OLEDs, which is being investigated in our laboratory.

Acknowledgment. We thank the Natural Sciences and Engineering Research Council and the Canada Foundation for Innovation for financial support and Dr. Igor Kozin for his assistance in recording the emission lifetimes of compounds **1–4**.

Supporting Information Available: Complete data of X-ray diffraction analyses for all structures, including tables of atomic coordinates, thermal parameters, bond lengths and angles, and hydrogen parameters. This material is available free of charge via the Internet at <http://pubs.acs.org>.

OM020220G